

## SOLUTION FOR SPILLWAY CHUTE AERATION THROUGH BOTTOM AERATORS

H. FUHRHOP<sup>2</sup>, H. E. SCHULZ<sup>1</sup> & H. WITTENBERG<sup>3</sup>

<sup>1</sup>University of São Paulo, Brazil.

<sup>2</sup>Delft University of Technology, The Netherlands.

<sup>3</sup>Leuphana Universität Lüneburg, Germany.

### ABSTRACT

Cavitation is a heavy threat for spillways with concrete chutes. Besides a proper design and execution, aeration is an effective means to avoid severe damages. A detailed study on bottom aerators of spillway chutes is presented here. Data from laboratory experiments were used to calibrate the coefficients of a physically based equation, which considers the effects of aerator geometry and different roughnesses of the surface of the aerator. After adjustment of scale factors, results computed by this equation showed a good agreement with observed data of different prototypes found in the literature. The main physical concepts of the developed equation are presented. The quantification of the air flow into the water jet was performed by separately considering the gas and liquid phases and using the subpressure under the jet of the aerator as a liaison between the two formulations. Consequently, this subpressure does not appear explicitly in the final formulation and does not need to be known for the quantification of the gas flow. The results show that the approach is suitable for the given problem.

*Keywords:* Aeration of channel flows, bottom aerators, designs of spillways.

### 1 INTRODUCTION

The study of bottom aerators in spillways is usually based on dimensional concepts complemented with semi-empirical assumptions and simplified theoretical approximations. Practical equations for the prediction of the air uptake can be presented as special cases of a more general nondimensional function, which involves a great number of parameters, as shown in the following equation:

$$\beta = \frac{Q_a}{Q_w} = f\left( \frac{V}{\sqrt{ge}}, \frac{Ve}{v}, \frac{V}{\sqrt{\Delta p/\rho_w}}, \frac{V}{\sqrt{\sigma/\rho_w L}}, \frac{L}{e}, \frac{L}{e}, \frac{\Delta y}{e}, \frac{d}{e}, \theta, \alpha, T \right) \quad (1)$$

Namely, the parameters are the ratio between the air flow rate and the water flow rate  $\beta = Q_a/Q_w$ , the Froude number  $Fr = V/\sqrt{ge}$ , the Reynolds number  $Re = Ve/v$ , the Weber number  $We = V/\sqrt{\sigma/\rho_w L}$ , geometrical relations  $L/e$ ,  $\Delta y/e$ ,  $d/e$ , characteristic slopes of the spillway  $\tan \theta$ ,  $\tan \alpha$ , and a parameter that quantifies the turbulence,  $T$ , but the definition of which is still open. The remaining variables are: density of air  $\rho_a$ , gravitational acceleration  $g$ , thickness of the water jet  $e$ , length of the water jet  $L$ , velocity of the water jet  $V$ , density of water  $\rho_w$ , surface tension  $\sigma$ , subpressure in the cavity beneath the lower nappe of the jet  $\Delta p$ , viscosity of water  $v$ , and the difference between the bottom levels of the chute before and after the aeration device  $d$  (offset, if present).  $\theta$  is the angle between the chute and the horizontal and  $\alpha$  is the angle between the chute and the ramp of the aerator.

The large number of parameters used to quantify the problem in eqn (1) may be still complemented by more variables, as shown in the subsequent formulation, and is one of the reasons because a more systematic approach to physically quantify aeration processes is still

not available. Despite this fact, several authors proposed interesting practical equations containing some of the shown nondimensional parameters (see, for example, [1–8]).

Dimensional analysis of empirical data leads generally to equations only valid for the used range of data. Hence, a significant uncertainty remains for the design when applying these equations on specific projects. Therefore, the study of a more general formulation to quantify the air uptake in bottom aerators was conducted at the School of Engineering at São Carlos, University of São Paulo, Brazil. The experiments were performed in the chute shown in Fig. 1, with a useful length of 5.0 m and a rectangular cross-section of 0.20-m wide and 0.50-m high. A broad data set was initially obtained by Carvalho [9] during laboratory experiments under controlled conditions. Furthermore, Lima [10] added concentration measurements to the hydraulic data and quantified the evolution of the air uptake along the jet formed by the bottom aerator (Lima *et al.* [11,12]). The inclination of the chute varied from 3° to 45° during the different sets of experiments. The chute aerator was composed of a ramp, which varied in length from 22.6 to 50.0 cm, forming an angle relative to the chute that varied from 0° to 10°. The aeration chamber under the jet had a depth of 0.12 m, width of 0.12m, and length of 0.18 m. The air discharge through the aeration chamber was measured using a bell-mouth nozzle at the entrance to the air supply pipe with an internal diameter of 0.0717 m (Fig. 3a and b). The air velocities were obtained from pressure measurements, using micro-manometers having one side open to the atmosphere and the other fixed in a pre-calibrated position in the pipe (Fig. 1). Lima [10] obtained mean air concentration profiles in the water jet formed at the aerator using a Cesium 137 probe (Figs 1 and 2). It allowed estimating the air detrainment at the end of the jet and a very detailed evolution of the air absorption along the lower nappe of the jet (for details, see Lima *et al.* [11]). The water flow rate measurements were performed using a rectangular weir located in the outlet channel and confirmed with an electromagnetic flow meter positioned in the inlet. The jet length from the aerator lip to the impact point was determined by the position of the highest measured pressure along the channel bottom in the region of jet reattachment. The pressure peaks were well defined. Figure 2 shows a sketch of the chute indicating several aspects of the experimental facilities. Table 1 shows the values adopted and the measured ranges of the most relevant parameters of this study.

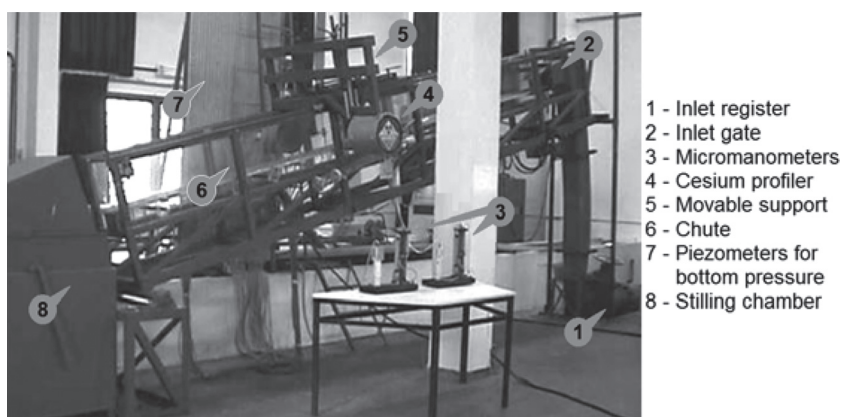


Figure 1: Chute used by Carvalho [9] and Lima [10] at the University of São Paulo, Brazil.

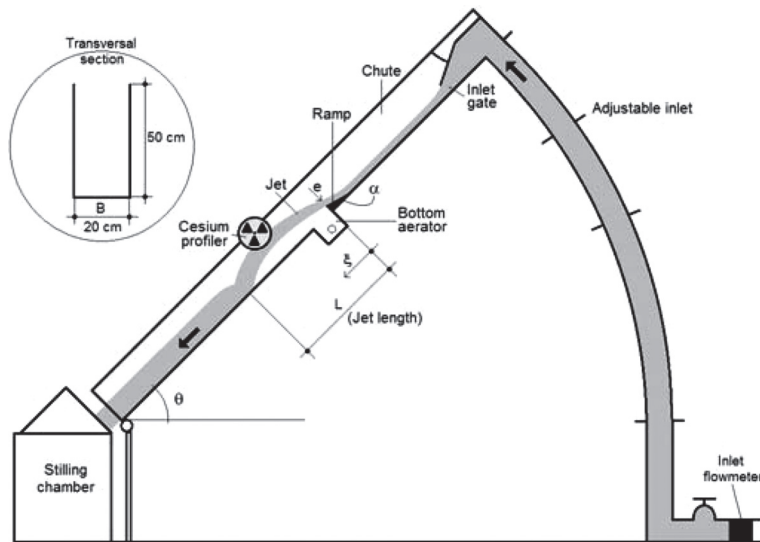


Figure 2: Sketch of the chute of Fig. 1, showing the aerator and variables used in the formulation.

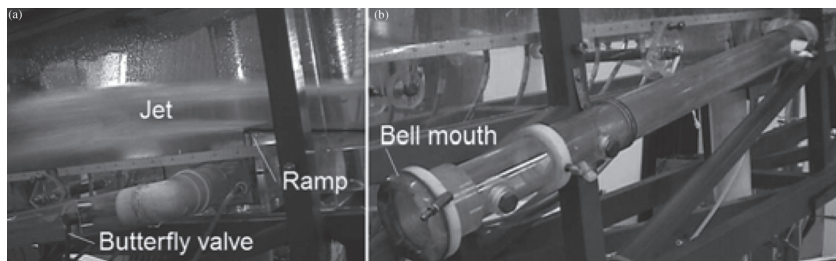


Figure 3: (a) Water jet forming at the end of the ramp and (b) air inlet structure showing the bell mouth at the entrance.

Table 1: Range of values of the different parameters measured in the chute of Fig. 1.

Parameter	Symbol	Range	Unit
Channel slope	$\theta$	0°, 3°, 14°, 30°, and 45°	Degree
Ramp inclination	$\alpha$	0°, 4°, 6°, 8°, and 10°	Degree
Butterfly valve opening	$\Psi$	15°, 30°, 45°, 60°, 75°, and 90°	Degree
Ramp step (or offset)	$D$	0.0 and 30.0	mm
Pressure difference	$\Delta p/\gamma$	0–52	mmWC
Jet length	$L$	0.42–2.92	m
Water flow	$Q_w$	38.8–185	l/s
Air flow	$Q_a$	3.5–55.5	l/s
Water depth	$e$	34–113	mm

The studies of Carvalho [9] and Lima [10] were continued by Arantes [13,14], who compared them with numerical predictions. Specific studies based on physical principles were then carried out sequentially (see [15–21]). It is recognized, in these studies, that the pressure beneath the water jet can hardly be determined ‘*a priori*’. The way followed to overcome this difficulty was to quantify the pressure considering the gaseous and the liquid phases separately. Two equations were obtained involving the subpressure, which could then be eliminated from the final equation, which contains parameters that are more directly obtained from experiments.

Conservation of mass, momentum, and energy were used to obtain the equation applied in the present study. However, the conservation principles depend, among others, on geometrical factors and on the energy dissipation rate, which still need empirical information and introduce coefficients that must be calibrated. The mathematical details to obtain the mentioned equation and the methodology to obtain the coefficients, as well as a first application to spillway prototypes, are described in detail in Schulz *et al.* [15], Brito *et al.* [16], and Fuhrhop [20]. To account for scaling effects, the approach of Kökpınar and Göğüs [6] was applied after Froude similitude had to be discarded following Schlurmann [22], who stated that due to high turbulence the transference from a model to a prototype is not possible with respect to air entrainment because of identical bubble rise velocities. This is also in agreement with Chanson and Murzyn [23], who came to the conclusion that dynamic similarity of two-phase flows in hydraulic jumps cannot be achieved with a Froude similitude. Hence, instead of Froude similitude, nonlinear regression was applied considering the approach of Kökpınar and Göğüs [6].

From the above considerations, the objective of the present study was to optimally adjust the mentioned physically based equation, furnishing details of this adjustment and a final equation that also considers scale effects, allowing its use for design purposes.

## 2 DETAILS OF THE APPLIED EQUATIONS

The sequence of equations of this item is based on the sequence of Schulz *et al.* [15].

### 2.1 Gaseous phase

Figure 4 shows a longitudinal cross-section of a spillway with water flowing over an aeration device (in gray) as well as the flow of entrained air (hatched). The assumed control volume for air flow is emphasized in the figure.  $Q_a$  and  $Q_w$  represent the flows of air and water, respectively.  $V_C$  is the air flow velocity in the inlet tube with length  $C$ .  $A$  is the sectional area,  $V$  is the velocity, and  $p$  is the pressure. The indices 0,  $E$ , and  $S$  refer to the atmospheric reference in a distant point, at the entrance, and at the exit of the control volume (at the cavity), respectively.

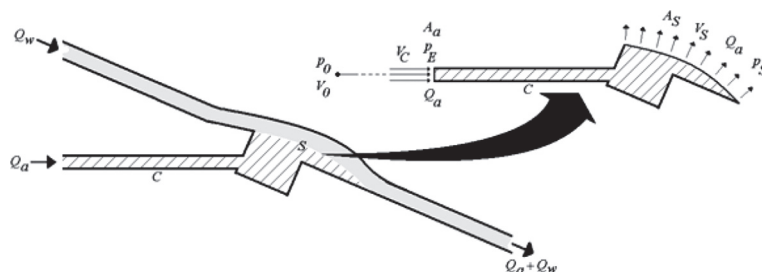


Figure 4: Control volume of the gaseous phase.

The equations of conservation of mass and energy are considered in their integral form and for steady conditions (Fox and McDonald [24]):

$$\int_{CS} \rho_a \vec{V}_a \cdot d\vec{A} = 0 \quad (2a)$$

$$\dot{Q} - \dot{W} = \int_{CS} \left( \frac{V_a^2}{2} + gz + \frac{p}{\rho_a} + u \right) \rho_a \vec{V}_a \cdot d\vec{A} \quad (2b)$$

$V_a$  is the air flow velocity,  $\dot{Q}$  and  $\dot{W}$  are the heat generated and the power realized by the system,  $z$  is an elevation,  $u$  is the internal energy, and  $CS$  indicates the control surface. After integration over the control volume, considering the outlet area  $A_S = \omega_0 L B$  ( $\omega_0$  is a coefficient that corrects for the curvature of the water jet and the irregularities due to turbulence), local and distributed losses of energy, neglecting elevation differences and observing the relation  $p_E = p_0 - \rho V_C^2/2$  (Fig. 4, see Schulz *et al.* [15] for details), it follows that:

$$V_C = V_S \frac{\omega_0 LB}{A_a} \quad (3a)$$

$$\frac{p_0 - p_S}{\rho_a g} = \frac{\Delta p}{\rho_a g} = \frac{V_S^2}{2g} + \frac{V_C^2}{2g} \left( 1 + k + f \frac{C}{D} \right) \quad (3b)$$

where  $B$  is the width of the channel,  $D$  is the diameter of the tube,  $k$  is a constant that quantifies the local losses, and  $f$  is the Darcy–Weisbach resistance factor (see, for example, Fox and McDonald [24]). Combining eqns (3a) and (3b), initially isolating the pressure difference and afterwards the air flow (the parameter of interest for the design), the two new equations read, respectively:

$$\Delta p = \frac{\rho_a V_S^2}{2} \left[ 1 + \frac{\omega_0^2 L^2 B^2}{A_a^2} c_R \right] \quad (4a)$$

$$Q_a = \omega_0 LB \frac{A_a}{A_w} \sqrt{\frac{2\Delta p}{\rho_a} \frac{1}{\left[ \left( \frac{A_a}{A_w} \right)^2 + c_R \left( \frac{\omega_0 L}{e} \right)^2 \right]}} \quad (4b)$$

$C_R = 1 + k + fL/D$  accounts for the losses in the inlet tube. By knowing  $\Delta p$  and the geometry of air and water flows, the air uptake can be rapidly obtained. However, the designer has no ‘a priori’ knowledge of  $\Delta p$ . As a consequence, equations involving explicitly the subpressure  $\Delta p$  are not useful for hydraulic design in engineering projects. Hence, a second equation to calculate  $\Delta p$  is needed in order to substitute this variable by more adequate flow parameters. This is attained by considering the liquid phase.

## 2.2 Liquid phase

Figure 5a shows a ‘slice’ of the water jet flowing over the aeration device. This approach is made to quantify forces and obtain the accelerations of flow in the  $x$  and  $y$  directions.

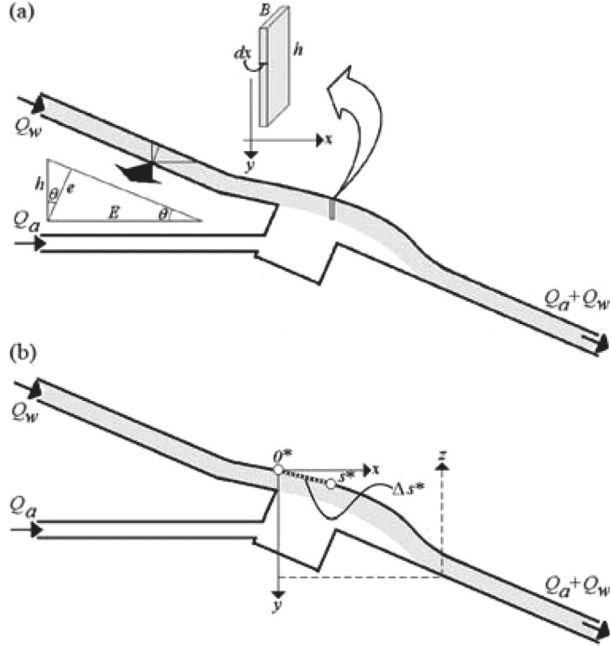


Figure 5: (a) Water jet flowing over the aeration device (in gray). (b) Local coordinate system with a flow path line along the upper jet surface for energy loss analysis.

For the  $x$ -direction, the force acting on the slice is given by

$$m a_x = F_x = \frac{\partial p}{\partial x} dx B h \quad (5)$$

where  $m$  is the mass of the water slice,  $a_x$  and  $F_x$  are the  $x$ -components of acceleration and force, respectively,  $e$  is the transversal thickness of the water jet,  $h$  being its vertical thickness, and  $E$  its horizontal thickness. To account for the distortional and dissipative effects of turbulence, a correction factor  $\omega_1$  was introduced. To create an applicable design tool,  $\partial p / \partial x \sim -\Delta p / E$  was assumed. The coefficient  $\omega_1$  considers the effects of this simplification leading to the following horizontal acceleration:

$$a_x = -\omega_1 \frac{\Delta p}{\rho_w E} \quad (6)$$

Similar steps were followed for the  $y$ -direction also considering gravitational acceleration, resulting in

$$a_y = g + \omega_2 \frac{\Delta p}{\rho_w h} \quad (7)$$

where  $a_y$  is the acceleration component in  $y$ -direction. Applying the Navier–Stokes equations to the water jet assuming steady flow, pressure gradients expressed by  $\Delta p/E$  and  $\Delta p/h$ ,

velocities varying as  $V_x = V_x(x)$  and  $V_y = V_y(y)$ , no relevant viscosity effects, and turbulence effects inserted into  $\omega_1$  and  $\omega_2$ , eqns (8a) and (8b) are obtained for the kinetic energy per unit mass in the  $x$  and  $y$  directions, respectively (see Schulz *et al.* [15], for details):

$$V_x \frac{\partial V_x}{\partial x} = -\omega_1 \frac{\Delta p}{\rho_w E} \quad \Rightarrow \quad V_x^2 = V_{0x}^2 - 2\omega_1 \frac{\Delta p}{\rho_w E} \Delta x \quad (8a)$$

$$V_y \frac{\partial V_y}{\partial y} = g + \omega_2 \frac{\Delta p}{\rho_w h} \quad \Rightarrow \quad V_y^2 = V_{0y}^2 + 2 \left( g + \omega_2 \frac{\Delta p}{\rho_w h} \right) \Delta y \quad (8b)$$

Equations (8a) and (8b) show that the evolution of the jet depends on the accelerations given by eqns (6) and (7), which depend on  $\Delta p$ . The ‘Bernoulli equation with losses’ (Fox and McDonald [24]) was then applied along a line at the upper surface of the jet, between the points  $0^*$  and  $s^*$  sketched in Fig. 5b. For uniform water velocities at the cross-sections, it leads to

$$z_{0^*} - z_{s^*} + \frac{V_{0^*}^2}{2g} - \frac{V_{s^*}^2}{2g} = \Delta h_f \quad (9)$$

$\Delta h_f$  is the head loss, and Fig. 5b shows that  $z_{0^*} - z_{s^*} = \Delta y$ . The total kinetic energy of the jet at  $0^*$  and  $s^*$  is obtained by summing up the kinetic energy of the  $x$ - and  $y$ -components of eqns (8a) and (8b). Thus, combining eqns (8) and (9) with these considerations and solving for  $\Delta p$  leads to

$$\Delta p = \frac{\rho_w g \Delta h_f}{\left( \omega_1 \frac{\Delta x}{E} - \omega_2 \frac{\Delta y}{h} \right)} \quad (10)$$

Equation (10) furnishes the subpressure at the aerator induced by the water jet. The Darcy–Weisbach equation (see, for example, Fox and MacDonald [24]) was used to determine  $\Delta h_f = f \Delta s^* V^2 / (2g D_H)$ , where  $f$  is the friction factor. The hydraulic diameter  $D_H$  was taken, as for wide rectangular channels,  $D_H = 4e$ . Figure 5a shows that  $h = e/\cos \theta$  and  $E = e/\sin \theta$ . Hence, eqn (10) was rewritten as

$$\Delta p = \frac{(f/8) \rho_w V^2}{\left( \omega_1 \frac{\Delta x}{\Delta s^*} \sin \theta - \omega_2 \frac{\Delta y}{\Delta s^*} \cos \theta \right)} \quad (11)$$

Equation (11) still represents a general solution. In this study, the geometric ratios  $\Delta x / \Delta s^*$ ,  $\Delta y / \Delta s^*$  and the velocity  $V$  were defined at  $x = 0$ , that is

$$\left. \frac{\Delta x}{\Delta s^*} \right|_{x=0} = \cos(\theta - \alpha), \quad \left. \frac{\Delta y}{\Delta s^*} \right|_{x=0} = \sin(\theta - \alpha), \quad V^2 = V^2 \Big|_{x=0} = V_o^2 \quad (12)$$

Different aerators may need different definitions for the geometrical parameters. Eqns (11) and (12) yield

$$\Delta p = \frac{(f/8)\rho_w V_0^2}{(\omega_1 \cos(\theta - \alpha) \sin \theta - \omega_2 \sin(\theta - \alpha) \cos \theta)} \quad (13)$$

Equation (13) contains only measurable parameters and thus allows the determination of  $\Delta p$  based on the liquid phase.

### 2.3 Air discharge

Equations (4b) and (13) furnish the discharge of the entrained air in the water jet, expressed as a function of easily measurable variables. The subpressure, in fact, causes the air movement but does not appear explicitly in the final equation. The mentioned equations lead to

$$\beta = \omega_6 \sqrt{\frac{\rho_w}{\rho_a} \frac{L}{e} \frac{A_a}{A_w}} \sqrt{\frac{1}{\left[ \left( \frac{A_a}{A_w} \right)^2 + \omega_7 \left( \frac{L}{e} \right)^2 \right]}} \sqrt{\frac{1}{[\omega_8 \sin \theta \cos(\theta - \alpha) - \sin(\theta - \alpha) \cos \theta]}} \quad (14)$$

The coefficients  $\omega_6$ ,  $\omega_7$ , and  $\omega_8$  result from algebraic operations on  $\omega_0$ ,  $\omega_1$ ,  $\omega_2$ ,  $C_R$ , and  $f$  (the latter two assumed to be constant for turbulent flows), showing that only three coefficients need to be adjusted based on experimental data.  $\omega_8$  expresses the relative importance of forces in  $x$ - and  $y$ -directions along the water jet;  $\omega_7$  represents the importance of the energy losses within the air duct (head losses), and  $\omega_6$  accounts for the proportionality between  $\beta$  and the global expression. As already mentioned, the coefficients can depend on the geometry details of the aeration device.

Equation (14) was presented by Schulz *et al.* [15], and the first values for the coefficients are encountered in Refs. [17–19]. Fuhrhop [20] conducted a more detailed analysis of the influence of different geometrical characteristics of the aeration device and subsequently adjusted the coefficients  $\omega_6$ ,  $\omega_7$ , and  $\omega_8$ , obtaining a good final correlation.

### 3 STATISTICAL ANALYSIS AND EFFECTS OF GEOMETRY

Brito and Schulz [19] suggested coefficients  $\omega_6$ ,  $\omega_7$ , and  $\omega_8$  for aeration devices having a smooth ramp and without step (or offset), as presented in eqn (15). The coefficients were fitted by the least-squares method using Excel®

$$\beta = \frac{1.4}{10^4} \sqrt{\frac{\rho_w}{\rho_a} \frac{L}{e} \frac{A_a}{A_w}} \sqrt{\frac{1}{\left[ \left( \frac{A_a}{A_w} \right)^2 + \frac{2.63}{100} e^{-\frac{8.5}{100}\psi} \left( \frac{L}{e} \right)^2 \right]}} \sqrt{\frac{1}{[1.043 \sin \theta \cos(\theta - \alpha) - \sin(\theta - \alpha) \cos \theta]}} \quad (15)$$

$\psi$  represents the opening angle of a butterfly valve positioned in the air duct, which simulates different head losses. The opening angles tested by Carvalho [9] were 15°, 30°, 45°, 60°, 75° and 90° (see Table 1; 90° represents a total opening). Further, Brito [17] and Brito and Schulz [19] tested this equation for prototypes, using the scaling factors suggested by Kökpinar and Göğüs [6], presented as,  $\beta_{prot} = \xi'' (\beta_{lab})^{\varepsilon''}$  where  $\xi'' (= 4.186)$  and  $\varepsilon'' (= 1.388)$  are the mentioned scaling factors. Adequate results were obtained for prototypes with data available in the literature [1,2,5].

Fuhrhop [20] used the data of Carvalho [9] for aeration devices with both, smooth and rough ramp surfaces, with and without step, and the general procedure followed by Brito *et al.* [16]. It was verified that the quadratic error function incorporating eqn (14) and the data of Carvalho [9] produced several local minima instead of a single global minimum, as shown in Fig. 6. In this figure, the results depend on variations of two coefficients. This led to an adjustment in successive steps using Excel® and the Quasi-Newton method in a multivariate optimization. The squared error was defined as the objective function to be optimized depending on the three already indicated coefficients. First adjustments were made to obtain fixed coefficients values as starting values. The data of smooth ramp surfaces, without step and with fully opened butterfly valve, were used first ( $\psi = 90^\circ$ ).

The data were analyzed for every combination of chute and ramp slopes ( $\theta = 3^\circ, 14^\circ, 30^\circ$  and  $45^\circ$  and  $\alpha = 4^\circ, 6^\circ, 8^\circ$  and  $10^\circ$ , respectively). Carvalho [9] demonstrated that deviations of the air flow rate were more probable at the lower rates. Although carefully controlled, eventual random deviations could lead to biased results of these lower values, generating outliers. The Grubbs' analysis for outliers was applied with a level of significance of 0.05 (details in Fuhrhop [20]), and the outliers were removed from the data set in the subsequent procedures (they were inserted in the graphs at the end of the analysis, for comparison). The new data set was optimized again (least-squares method), resulting in new coefficient values. In the following, based on the analysis of  $\omega_7$  presented by Schulz *et al.* [15], an empirical exponential adjustment was made, leading to the results shown in Fig. 7a. The adjusted data for smooth ramps of the bed aerator without step (or offset), for all opening angles of the butterfly valve  $\psi$ , for all combinations of  $\alpha$  and  $\theta$  and without outliers is presented in Fig. 7b. The adjusted coefficients were  $\omega_6 = 3.507 \cdot 10^{-4}$ ,  $\omega_7 = 0.0204 e^{0.041\psi}$  and  $\omega_8 = 1.175$ , deviating from the values presented in eqn (15), though still in the range of those values. Figure 7b shows a cohesive cloud of data. The coefficient of determination between data and prediction was  $R^2 = 0.843$ , the standard deviation was 0.271, and the quantity of outliers was 7.2% in this first analysis, a value that was reduced in the final analysis.

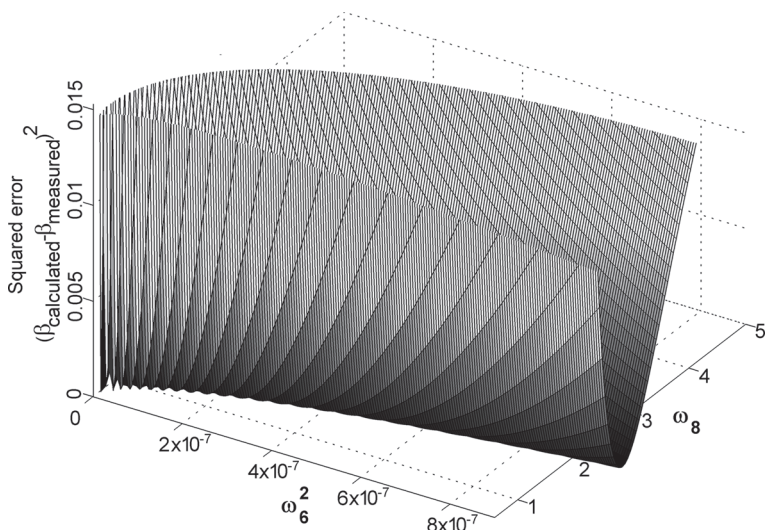


Figure 6: Multiple local minima of the objective function as dependent on  $\omega_6^2$  and  $\omega_8$ .  $\omega_6$  is squared because it was inserted into the last square root of eqn (14).

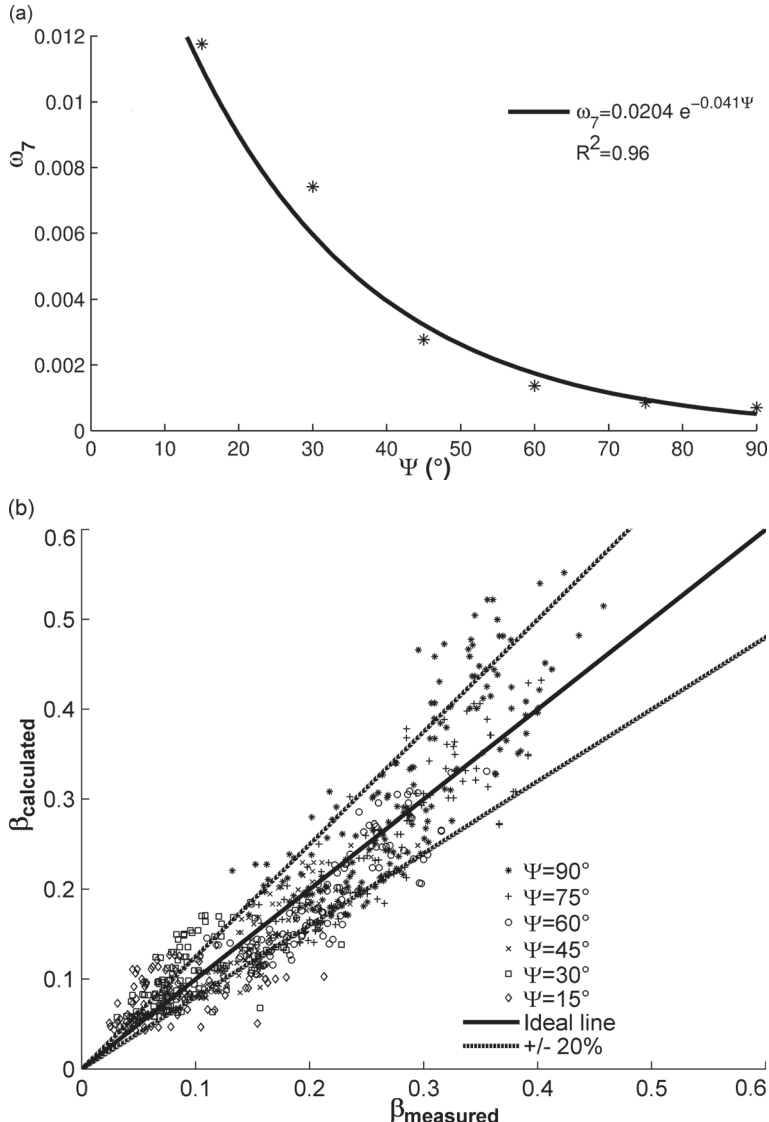


Figure 7: (a)  $\omega_7$  versus opening angle of the valve ( $\psi$ ). (b) Measured and calculated  $\beta$  (eqn 14) for smooth ramps without step (details in Fuhrhop [20], data from Carvalho [9]).

The geometrical variations related to the roughness of the ramp and the presence of a step (offset) were then investigated (Fig. 8). The step (offset) used for all ramps had a height of 3.0 cm. A sensitivity analysis showed that  $\omega_6$  was the coefficient most influenced by these variations. Thus,  $\omega_7$  and  $\omega_8$  kept their functional form and values from the previous adjustments. For simplicity,  $\omega_6$  was inserted into the last square root of eqn (14). In the sequence of this analysis,  $\omega_6$  appears squared, that is  $\omega_6^2$ .

The effect of roughness was evaluated by calculating  $\beta$  for each diameter of sand,  $s'$  ( $s'$  = maximum diameter of the sand glued to the ramp surface). A linear dependence between  $\omega_6^2$  and  $s'$  was observed for bed aerators without step. However, the combined effect of rough-

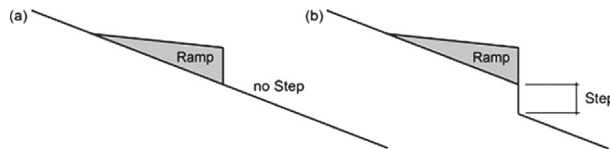


Figure 8: (a) Longitudinal profile of chute without step (offset). (b) Profile of chute with step.

ness, chute angles, ramp angles, and step led to a nonlinear dependence between  $\omega_6^2$  and these variables.

To account for both observed effects (step and  $s'$ ), the functional form (16a) was proposed, involving the linear dependence with  $s'$  and a nonlinear function of the remaining parameters. For the nonlinear function, a truncated series (second-degree polynomial) of the angle of the ramp ( $a$ ) was multiplied by a factor accounting for the presence of the step ( $d'$ ) and a factor involving a power of the angle of the chute ( $\theta$ ).  $\omega_6^2$  was quantified as

$$\omega_6^2 = m * s' + f(d', \theta, a) \quad (16a)$$

$$\omega_6^2 = m * s' + d' \theta^{n^*} (a^* + b * a + c * a^2) \quad (16b)$$

The constants  $a^*$ ,  $b^*$ ,  $c^*$ ,  $m^*$ , and  $n^*$  were adjusted for all experimental data.  $d'$  assumed the value 0.752 for the aerator with step, and 1.0 for the aerator without step, considering the present data. The two values derive from the fact that only one step height was tested experimentally (3.0 cm, see Table 1). The dimensions used were:  $[s'] = \text{mm}$ ,  $[a] = \text{rad}$ ,  $[\theta] = \text{rad}$ . The best-fitted solution is given by eqn (17):

$$\beta = \sqrt{\frac{\rho_w}{\rho_a} \left( \frac{L}{e} \frac{A_a}{A_w} \right)^2} \sqrt{\frac{[0.159s' + \theta^{0.26}(1.11 + 2.24a)d']10^{-7}}{\left[ \left( \frac{A_a}{A_w} \right)^2 + \frac{2.04}{100} e^{-\frac{4.1}{100}\psi} \left( \frac{L}{e} \right)^2 \right] \sqrt{[1.175 \sin \theta \cos(\theta - a) - \sin(\theta - a) \cos \theta]}}} \quad (17)$$

Due to eqns (16a) and (16b), the final equation has a semi-empirical characteristic. However, it must be emphasized that the theoretical analysis led to the general eqn (14), which physical basis allowed defining the coefficients necessary for the fine adjustments based on empirical data. Hence, the physically based theoretical analysis is fundamental for obtaining a causal equation for the air uptake. The comparison between measured and computed data with eqn (17) is shown in Fig. 9. The outliers were also included in the figure, showing that their deviations are significant for smaller values of  $\beta$ . Figure 9 also shows that the ramp roughness increases the value of  $\beta$ , which is well-reproduced by the proposed model. On the other hand, the presence of a step (offset) did not show observable variations or impacts on the air entrainment process. About 6% of the data were rejected as outliers by Grubbs analysis (i.e. only 96 values in a total of 1537). To extend the present result, the experimental values of Table 1, taken from Carvalho [9], express the limits of the adjusted coefficients. The obtained coefficient of determination was  $R^2 = 0.88$ .

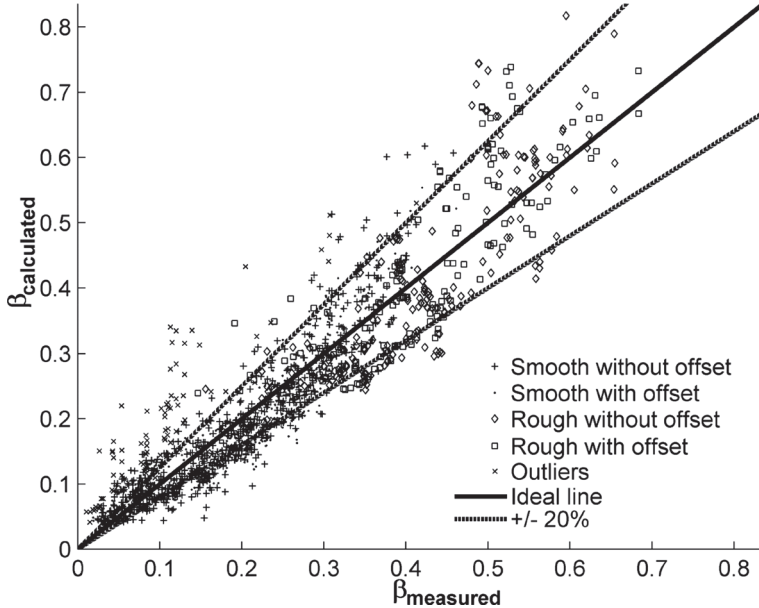


Figure 9: Measured and calculated  $\beta$  for all angles, roughnesses, and steps (offsets). Outliers are indicated by  $x$  (data from Carvalho [9]).

#### 4 APPLICATION ON PROTOTYPES

Ideally, equations obtained through models should be applied also on prototypes. However, scaling factors must generally be considered because a perfect similarity between different scales is most often unachievable. As already mentioned, Kökpınar and Göğüs [6] suggested a corrective relation  $\beta_{prot} = \xi''(\beta_{lab})^{\varepsilon''}$ . The data of the dams of Emborcação and Foz de Areia, Brazil (furnished by Pinto [5]), allowed obtaining  $\xi'' = 1.9332$  and  $\varepsilon'' = 0.7606$ , and therewith closer to unity (ideal case) than the adjustments of Kökpınar and Göğüs [6] and Brito [17]. A ramp roughness of  $s' = 2.5\text{mm}$  (concrete without special treatment) was used together with an opening of  $60^\circ$  of the butterfly valve ( $\psi = 60^\circ$ ), accounting for losses in the inlet structure of the air flow. The achieved adjustments are presented in Fig. 10a and b. Details may be found in Fuhrhop [20]. With the adjusted scaling factors, the equation of  $\beta$  for prototypes is given by eqn (18):

$$\beta_{prot} = 1.9332(\beta_{lab})^{0.7606} \quad (18)$$

$\beta_{lab}$  is given by eqn (17). The good correlation obtained in Fig. 10 points to the adequacy of this formulation.

Equations (17) and (18) depend directly on  $L/e$ ,  $A_d/A_w$ ,  $s'$ ,  $a$  and  $\theta$ . The experimental ranges tested here were  $6.0 \leq L/e \leq 80$ ,  $0.20 \leq A_d/A_w \leq 0.59$ , and  $s'$ ,  $a$ ,  $\theta$  already furnished in Table 1. Furthermore,  $d' = 0.752$  or  $1.0$ . For design purposes, predictions of the water depth  $e$ , needed to calculate  $A_w$ , may be obtained from the usual S2 surface profiles (see Chow [25]), for which a theoretical solution is presented by Simões *et al.* [26]. Predictions of  $L/e$  may be obtained by applying the equation of Schwarz and Nutt [27], as suggested by Lima *et al.* [12].

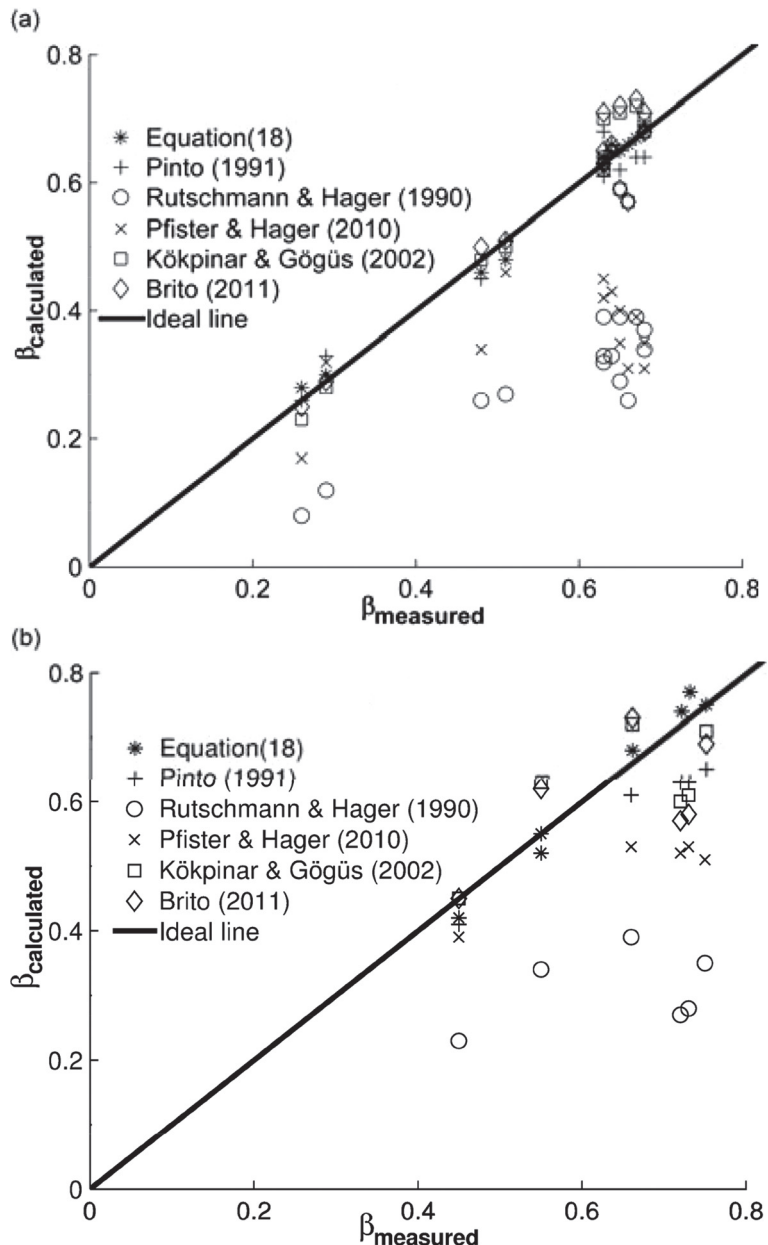


Figure 10: (a) Measured and calculated  $\beta$  for Emborcação dam.  $R^2 = 99.0\%$ . (b) The same for Foz de Areia dam.  $R^2 = 97.6\%$ . Predictions of Pinto [5], Kökpinar and Göğüs [6], and Brito [17] also adjust well to the data. Eqn (18) shows the best correlation (data from Pinto [5]).

## 5 CONCLUSIONS

A calibrated equation was provided that adequately reproduces data of air entrainment induced by water flow over bottom aerators. The equation considers a wide range of air and water discharges, water depths and roughness of the ramp surface, inclination of the chute and of the ramp of the aerator, head losses at the air inlet, and the presence of steps (offsets) at the aeration device. The equation was obtained following physical considerations that indicated where empirical adjustments are necessary. The adjustments were conducted by using the least-squares method and empirical functions for the coefficients, which relate them to the measured geometrical parameters. The experimental data were taken from the literature. Furthermore, scaling factors were adjusted for the present formulation, allowing reproducing the data of entrained air for two prototypes described in literature.

The ranges tested for the parameters of the formulation were  $6.0 \leq L/e \leq 80$ ,  $0.20 \leq A_d/A_w \leq 0.59$ ,  $d' = 0.752$  or  $1.0$ , and  $s'$ ,  $a$  and  $\theta$  furnished in Table 1.

The present equation has a good adherence to the measured data used in this study. Since it is also based on physical principles, the use of this equation in future studies and applications of air uptake in bed aerators is suggested.

## ACKNOWLEDGEMENTS

The second author thanks Prof. Fazal Hussain Chaudhry for his support to this research line at EESC/USP, and the Brazilian research support institutions CNPq, CAPES, and FAPESP.

## REFERENCES

- [1] Pinto, N.L.S., Neidert, S.H. & Ota, J.J., Aeration at high velocity flows. *Water Power and Dam Construction*, **34**(2), pp. 34–38; **34**(3), pp. 42–44, 1982.
- [2] Pinto, N.L.S. & Neidert, S.H., Evaluation of entrained air flow through aerators. *Water Power and Dam Construction*, **Aug.**, pp. 40–44, 1983.
- [3] Rutschmann, P. & Volkart, P., Spillway chute aeration. *Water Power and Dam Construction*, **Jan.**, pp. 10–15, 1988.
- [4] Rutschmann, P. & Hager, W.H., Air entrainment by spillway aerators. *Journal of Hydraulic Engineering*, **116**(6), pp. 765–782, 1990. doi: [http://dx.doi.org/10.1061/\(ASCE\)0733-9429\(1990\)116:6\(765\)](http://dx.doi.org/10.1061/(ASCE)0733-9429(1990)116:6(765))
- [5] Pinto, N.L.S., Prototype aerator measurements. *IAHR Hydraulic Structures Design Manual 4, Air Entrainment in Free-Surface Flow*, ed. Wood, Balkema: Rotterdam, pp. 115–130, 1991.
- [6] Kökpinar, M.A. & Göögüs, M., High-speed jet flows over spillway aerators. *Journal of Civil Engineering*, **29**, pp. 885–898, 2002.
- [7] Pfister, M. & Hager, W.H., Chute aerators II: hydraulic design. *Journal of Hydraulic Engineering*, **136**(6), pp. 507–518, 2010. doi: [http://dx.doi.org/10.1061/\(ASCE\)HY.1943-7900.0000201](http://dx.doi.org/10.1061/(ASCE)HY.1943-7900.0000201)
- [8] Falvey, H.T., Discussion of “air uptake along the lower nappe of a spillway aerator”. *Journal of Hydraulic Research*, **47**(5), pp. 683–684, 2009.
- [9] Carvalho, P.D., *Aeration of High-speed Flows in Chutes with Large Slopes* (Aeração de Escoamentos de Alta velocidade em Canais de Forte Declividade – in Portuguese). Doctor thesis. School of Engineering at São Carlos, University of São Paulo, Brazil, 1997.
- [10] Lima, A.C.M., *Determination of turbulent structures of aerated flows in chutes using PIV* (Caracterização da estrutura turbulenta em escoamentos aerados em canal de forte declividade com auxílio de técnicas de velocimetria a laser – in Portuguese). Doctor thesis. School of Engineering at São Carlos, University of São Paulo, Brazil, 2004.
- [11] Lima, A.C.M., Schulz, H.E. & Gulliver, J.S., Air uptake along the lower nappe of a spillway aerator. *Journal of Hydraulic Research*, **46**(6), pp. 839–843, 2008.

- [12] Lima, A.C.M., Schulz, H.E. & Gulliver, J.S., Discussion of “air uptake along the lower nappe of a spillway aerator”. *Journal of Hydraulic Research*, **47(5)**, pp. 683–684, 2009.
- [13] Arantes, E.J., *Stepped Spillways’ Flow Characterization using CFD Tools* (Caracterização do Escoamento sobre Vertedores em Degraus via CFD – in Portuguese). Doctor thesis. School of Engineering at São Carlos, University of São Paulo, Brazil, 2007.
- [14] Arantes, E.J., Porto, R.M., Gulliver, J.S., Lima, A.C.M. & Schulz, H.E., Lower nappe aeration in smooth channels: experimental data and numerical simulation. *Anais da Academia Brasileira de Ciências*, **82(2)**, pp. 521–537, 2010. doi: <http://dx.doi.org/10.1590/S0001-37652010000200027>
- [15] Schulz, H.E., Brito, R.J.R., Simões, A.L.A., Puche, A.A.S. & Lobosco, R.J., Theoretical models for analyses of bed aerators using physical principles (Modelos Teóricos para Análise de Aeração em Aeradores de Fundo Utilizando Princípios Físicos – in Portuguese), *Memorias del XXIV Congreso Latinoamericano de Hidráulica*. IAHR: Punta del Este, Uruguay, 13 pp, 2010.
- [16] Brito, R.J.R., Simões, A.L.A., Puche, A.A.S., Schulz, H.E. & Porto, R.M., Air uptake in high-velocity aerators in spillways: analyses of data and models (Incorporação de Ar por Aeradores de Escoamentos de Alta Velocidade em Vertedores: Análise de Dados e Modelos – in Portuguese). *Memorias del XXIV Congreso Latinoamericano de Hidráulica*, IAHR: Punta del Este, Uruguay, 11 pp, 2010.
- [17] Brito, R.J.R., *Analysis of aeration through bed aerators in high speed flows on weirs* (Análise da aeração em escoamento de alta velocidade em calhas de vertedores – in Portuguese). MSc dissertation. School of Engineering at São Carlos, University of São Paulo, Brazil, 2011.
- [18] Schulz, H.E. & Brito, R.J.R., Predicting aeration in spillways through bed aerators based on physical principles (Previsão da Aeração em Vertedores com o Uso de Aeradores de Fundo Fundamentada em Princípios Físicos – in Portuguese). *Proceedings, CLME 2011/III CEM*, Ed INEGI, Maputo, Moçambique, 15 pp., 2011.
- [19] Brito, R.J.R. & Schulz, H.E., Equations with physical bases for bed-aerator: analyses of data and models (Equações com Bases Físicas para Aerador de Fundo: Análise de Dados e Modelos – in Portuguese). *Proceedings, CLME 2011/III CEM*, Ed INEGI, Maputo, Moçambique, 15 pp, 2011.
- [20] Fuhrhop, H., *Spillway chute aeration – calibration of a physically based approach by using measured data*. Bachelor Thesis. Leuphana University Lüneburg, Germany, 2011.
- [21] Fuhrhop, H., Schulz, H.E. & Wittenberg, H., Solving bottom aerators in spillways (Solução para Aeradores de Fundo em Vertedores – in Portuguese), *Memorias del XXV Congreso Latinoamericano de Hidráulica*, IAHR, San José, Costa Rica, 10 pp, 2012.
- [22] Schlurmann, T., *Skriptum Wasserbauliches Versuchswesen*. Bergische Universität Wuppertal, Obering, p. 22, 2002.
- [23] Chanson, H. & Murzyn, F., Froude similitude and scaling effects affecting air entrainment in hydraulic jumps. *World Environmental and Water Resources Congress*, Ahupua'a, Hawaii, 10 pp, 2008.
- [24] Fox, R.W. & McDonald, A.T., Introduction to Fluid Mechanics (in Portuguese), ed. Guanabara Dois, Rio de Janeiro, 1981.
- [25] Chow, V.T., Open-Channel Hydraulics, McGraw Hill Book Company, New York, 1959.
- [26] Simões, A.L.A., Schulz, H.E. & Porto, R.M., Stepped and smooth spillways: resistance effects on stilling basin lengths. *Journal of Hydraulic Research*, **48(3)**, pp. 329–337, 2010. doi: <http://dx.doi.org/10.1080/00221686.2010.481853>
- [27] Schwarz, I. & Nutt, L.P., Projected Nappes subjected to transverse pressure. *Journal of Hydraulic Engineering ASCE*, **89(HY7)**, pp. 97–104, 1963.